PERGAMON

International Journal of Solids and Structures 36 (1999) 1701–1714

INTERNATIONAL JOURNAL OF SOLIDS and STRUCTURES

The in-plane loading of rigid disc inclusion embedded in a crack

A. P. S. Selvadurai*

Department of Civil Engineering and Applied Mechanics, McGill University, Montreal, QC., Canada H3A 2K6

Received 7 October 1997; in revised form 10 February 1998

Abstract

The paper examines the in-plane loading of a disc shaped rigid disc inclusion which is embedded in bonded contact with the plane surfaces of a penny-shaped crack. The mixed boundary value problem governing the elastostatic problem is reduced to the solution of a system of coupled integral equations, which are solved numerically to determine results of engineering interest. These results include the in-plane stiffness of the disc inclusion and the crack opening mode stress intensity factor at the boundary of the penny-shaped crack.

1. Introduction

The disc inclusion problem in the classical theory of elasticity is a particular simplification of the general category of three-dimensional inhomogeneities. When the physical configuration of the inhomogeneity allows its modelling as a disc inclusion, the analysis of the inclusion problem can be considerably simplified. Attention can be focused on the analysis of a variety of inclusion problems which are essentially mixed boundary value problems related to an elastic halfspace region. Elastostatic problems associated with disc inclusions have been successfully applied to examine a variety of problems of interest to the mechanics of multiphase composite materials and geomechanics. The investigations by Collins (1962), Keer (1965) and Kassir and Sih (1968) are the pioneering works in this area. Since these original developments, the theory of a disc inclusion has been applied to a variety of situations involving anchor-type objects used in geomechanical applications. These studies have taken into consideration non-classical effects such as material anisotropy, influence of bi-material regions, flexibility of the inclusion, delaminations and cracking both within and exterior to the inclusion region and the interaction between the inclusion and externally placed loads. Accounts of these developments are given by Mura (1981, 1988), and in the recent articles by Selvadurai et al. (1990), and Selvadurai (1994a, b).

* Fax: 00 514 398-7361; e-mail: apss@civil.lan.mcgill.ca

0020–7683/99/$ - see front matter © 1998 Elsevier Science Ltd. All rights reserved
PII: S0020–7683(98)00063–8

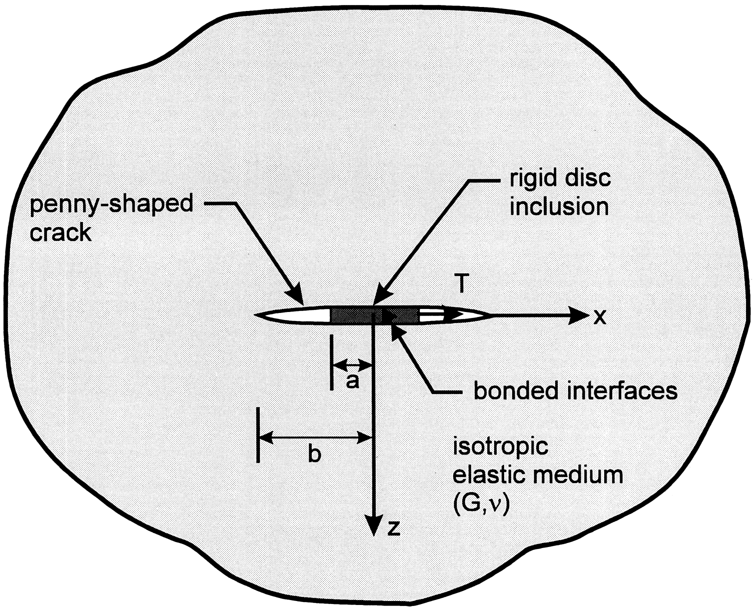

Fig. 1. In-plane translation of a rigid disc inclusion embedded in a penny-shaped crack.

In this paper we examine the problem related to a disc-shaped rigid circular inclusion which is embedded at the centre of a penny-shaped crack. The problem may be visualized either as a situation where fracturing has extended beyond the boundary of a rigid disc inclusion or where an inclusion region is created by the injection of a cementitious material into a geological medium by hydraulic facturing (Fig. 1). The disc inclusion embedded in a crack is, therefore, an approximate analogue of the anchor region. In general the rigid anchor region can be subjected to various modes of deformation. The axial loading of a rigid disc anchor embedded in complete bonded contact with the faces of the penny-shaped crack was examined by Selvadurai (1989). This result was extended by Selvadurai (1994b) to examine the case when the axial loading in the presence of delamination at one face of the inclusion.

In this study we extend the work to include the in-plane loading of the rigid circular disc inclusion for the particular case when the inclusion is in bonded contact with the faces of the penny-shaped crack. The in-plane loading of the inclusion is more consistent with situations where the anchorage is formed at orientations normal to a direction of minimum principal stress exerted, for example, by self weight stresses. Also, the problem examined considers the case where the rigid disc anchor or inclusion is located, in bonded contact, at the centre of the penny-shaped crack. Such positioning is expected to produce an anchorage of highest compliance, which is important to the assessment of the elastostatic efficiency of the anchorage. The mixed boundary value problem resulting from the anchor (inclusion)–crack interaction problem is reduced to the solution of a set of coupled integral equations which are solved in a numerical fashion. Numerical results are presented for the in-plane stiffness of the inclusion and for the crack opening mode stress intensity factor at the boundary of the penny-shaped crack.

2. Governing equations

The associated asymmetric elastostatic boundary value problem can be formulated by employing the stress function techniques developed by Muki (1960). The stress functions are governed by the differential equations

$$\nabla^2\nabla^2\Phi(r,\theta,z) = 0 \tag{1a}$$

$$\nabla^2\Psi(r,\theta,z) = 0 \tag{1b}$$

where

$$\nabla^2 = \frac{\partial^2}{\partial r^2} + \frac{1}{r}\frac{\partial}{\partial r} + \frac{1}{r^2}\frac{\partial^2}{\partial\theta^2} + \frac{\partial^2}{\partial z^2} \tag{2}$$

is Laplace's operator referred to the cylindrical polar coordinate system. The displacement and stress components in the elastic medium can be expressed in terms of the functions $\Phi(r,\theta,z)$ and $\Psi(r,\theta,z)$. Considering a Hankel transform development of the governing equations we can show that the relevant solutions applicable to the region $0 \leqslant z < \infty$ take the forms

$$\Phi(r,\theta,z) = \cos\theta\int_0^\infty \xi[A(\xi)+zB(\xi)]\,e^{-\xi z}J_1(\xi r)\,\mathrm{d}\xi \tag{3}$$

$$\Psi(r,\theta,z) = \sin\theta\int_0^\infty \xi C(\xi)\,e^{-\xi z}J_1(\xi r)\,\mathrm{d}\xi \tag{4}$$

where $A(\xi)$, $B(\xi)$ and $C(\xi)$ are arbitrary functions. The displacement and stress components relevant to the formulation of the boundary value problem can be obtained, from (3) and (4), in the forms

$$2Gu_r(r,\theta,z) = \frac{\cos\theta}{r}\int_0^\infty [\xi\{\xi A(\xi)-B(\xi)(1-\xi z)\}\{\xi rJ_0(\xi r) - J_1(\xi r)\}+2\xi C(\xi)J_1(\xi r)]\,e^{-\xi z}\,\mathrm{d}\xi \tag{5}$$

$$2Gu_\theta(r,\theta,z) = \frac{\sin\theta}{r}\int_0^\infty [\xi\{-\xi A(\xi)+(1-\xi z)B(\xi)\}J_1(\xi r) - 2\xi C(\xi)\{r\xi J_0(\xi r)-J_1(\xi r)\}]\,e^{-\xi z}\,\mathrm{d}\xi \tag{6}$$

$$2Gu_z(r,\theta,z) = -\cos\theta\int_0^\infty \xi^2[\xi A(\xi)+B(\xi)\{\xi z+2(1-2\nu)\}]\,e^{-\xi z}J_1(\xi r)\,\mathrm{d}\xi \tag{7}$$

and

$$\sigma_{zz}(r,\theta,z) = \cos\theta\int_0^\infty [\xi^4A(\xi)+B(\xi)\{(1-2\nu)\xi^3+\xi^4 z\}]\,e^{-\xi z}J_1(\xi r)\,\mathrm{d}\xi \tag{8}$$

$$\sigma_{\theta z}(r,\theta,z) = \frac{\sin\theta}{r}\left[\int_0^\infty \xi\{\xi^2 A(\xi)+B(\xi)(\xi^2 z-2v\xi)\}\, e^{-\xi z} J_1(\xi r)\,\mathrm{d}\xi \right.$$
$$\left. + \int_0^\infty \xi^2 C(\xi)\{\xi r J_0(\xi r)-J_1(\xi r)\}\, e^{-\xi z}\,\mathrm{d}\xi\right] \quad (9)$$

$$\sigma_{rz}(r,\theta,z) = \frac{\cos\theta}{r}\left[\int_0^\infty \xi\{-\xi^2 A(\xi)+(2v\xi-\xi^2 z)B(\xi)\}\{\xi r J_0(\xi r)-J_1(\xi r)\}\, e^{-\xi z}\,\mathrm{d}\xi \right.$$
$$\left. - \int_0^\infty \xi^2 C(\xi) J_1(\xi r)\, e^{-\xi z}\,\mathrm{d}\xi\right] \quad (10)$$

where G is the linear elastic shear modulus and v is Poisson's ratio.

3. The disc inclusion problem

We consider the problem of a rigid circular disc inclusion of radius 'a' which is embedded in bonded contact with the surfaces of a penny-shaped crack of radius 'b'. The inclusion is subjected to an in-plane force of magnitude T which induces a rigid body displacement 'δ' in the plane of the inclusion. The problem exhibits symmetry about the plane $z = 0$. Consequently, the problem can be formulated as a mixed boundary value problem related to a halfspace region $0 \leqslant z < \infty$. The mixed boundary conditions applicable to the crack–inclusion interaction problem are as follows; with displacement boundary conditions

$$u_r(r,\theta,0) = \delta\cos\theta; \quad 0 \leqslant r \leqslant a \quad (11)$$

$$u_\theta(r,\theta,0) = -\delta\sin\theta; \quad 0 \leqslant r \leqslant a \quad (12)$$

$$u_z(r,\theta,0) = 0; \quad 0 \leqslant r \leqslant a; \quad b \leqslant r < \infty \quad (13)$$

and traction boundary conditions

$$\sigma_{rz}(r,\theta,0)\sin\theta+\sigma_{\theta z}(r,\theta,0)\cos\theta = 0; \quad a < r < \infty \quad (14)$$

$$\sigma_{rz}(r,\theta,0)\cos\theta-\sigma_{\theta z}(r,\theta,0)\sin\theta = 0; \quad a < r < \infty \quad (15)$$

$$\sigma_{zz}(r,\theta,0) = 0; \quad a < r < b \quad (16)$$

Using the integral representations (5)–(10) for the displacement and stress components, the boundary conditions (11)–(16) can be effectively reduced to the following system of integral equations:

$$\int_0^\infty \left[L(\xi)-\frac{M(\xi)}{(7-8v)}-\frac{2(1-2v)}{(7-8v)}N(\xi)\right]J_0(\xi r)\,\mathrm{d}\xi = \frac{16G\delta(1-v)}{(7-8v)}; \quad 0 \leqslant r \leqslant a \quad (17)$$

$$\int_0^\infty \left[M(\xi)-\frac{L(\xi)}{(7-8v)}-\frac{2(1-2v)}{(7-8v)}N(\xi)\right]J_2(\xi r)\,\mathrm{d}\xi = 0; \quad 0 \leqslant r \leqslant a \quad (18)$$

$$\int_0^\infty N(\xi)J_1(\xi r)\,\mathrm{d}\xi = 0\,; \quad 0 \leqslant r \leqslant a \tag{19}$$

$$\int_0^\infty N(\xi)J_1(\xi r)\,\mathrm{d}\xi = 0\,; \quad b < r < \infty \tag{20}$$

$$\int_0^\infty \xi L(\xi)J_0(\xi r)\,\mathrm{d}\xi = 0\,; \quad a < r < \infty \tag{21}$$

$$\int_0^\infty \xi M(\xi)J_2(\xi r)\,\mathrm{d}\xi = 0\,; \quad a < r < \infty \tag{22}$$

$$\int_0^\infty \xi\left[L(\xi)+M(\xi)+\frac{2N(\xi)}{(1-2\nu)}\right]J_1(\xi r) = 0\,; \quad a < r < b \tag{23}$$

where the functions $L(\xi)$, $M(\xi)$ and $N(\xi)$ are related to the functions $A(\xi)$, $B(\xi)$ and $C(\xi)$ according to

$$2\xi^3(1-\nu)A(\xi) = 2\nu N(\xi)+(1-2\nu)\{L(\xi)+M(\xi)\} \tag{24}$$

$$4\xi^2(1-\nu)B(\xi) = 2N(\xi)-L(\xi)-M(\xi) \tag{25}$$

$$2\xi^2 C(\xi) = L(\xi)-M(\xi) \tag{26}$$

Considering the integral equations (17)–(23) we introduce the following representations

$$L(\xi) = \int_0^a \varphi_1(t)\cos(\xi t)\,\mathrm{d}t = \frac{\varphi_1(a)\sin(\xi a)}{\xi} - \frac{1}{\xi}\int_0^a \varphi'(t)\sin(\xi t)\,\mathrm{d}t \tag{27}$$

$$M(\xi) = \int_0^a t\varphi_2(t)J_2(\xi t)\,\mathrm{d}t \tag{28}$$

with $\varphi_1(0) = 0$ and the prime denotes the derivative of the function with respect to t. Substituting (27) and (28) into (21) and (22) we find that both equations are identically satisfied. Substituting (27) into (17) we obtain

$$\int_0^r \frac{\varphi_1(t)\,\mathrm{d}t}{(r^2-t^2)^{1/2}} = \frac{16G\delta(1-\nu)}{(7-8\nu)} + \int_0^\infty \left[\frac{M(\xi)}{(7-8\nu)} + \frac{2(1-2\nu)N(\xi)}{(7-8\nu)}\right]J_0(\xi r)\,\mathrm{d}\xi\,; \quad 0 < r < a \tag{29}$$

which is an integral equation of the Abel type, the solution of which is given by

$$\varphi_1(t) = \frac{32G\delta(1-\nu)}{(7-8\nu)\pi} + \frac{2}{\pi(7-8\nu)}\int_0^\infty [M(\xi)+2(1-2\nu)N(\xi)]\cos(\xi t)\,\mathrm{d}\xi\,; \quad 0 < t < a \tag{30}$$

The eqn (23) can be written in the form

$$\int_0^\infty \xi N(\xi) J_1(\xi r)\,\mathrm{d}\xi = -\frac{(1-2\nu)}{2}\int_0^\infty \xi[L(\xi)+M(\xi)]J_1(\xi r)\,\mathrm{d}\xi\,; \quad a<r<b \tag{31}$$

We assume that (31) admits a representation

$$\int_0^\infty \xi N(\xi) J_1(\xi r)\,\mathrm{d}\xi = \begin{cases} f_1(r)\,; & 0<r<a \\ f_2(r)\,; & a<r<b \\ f_3(r)\,; & b<r<\infty \end{cases} \tag{32}$$

With the help of Hankel transforms, we obtain from (31) and (32)

$$N(\xi) = \int_0^a rf_1(r)J_1(\xi r)\,\mathrm{d}r + \int_a^b rf_2(r)J_1(\xi r)\,\mathrm{d}r + \int_b^\infty rf_3(r)J_1(\xi r)\,\mathrm{d}r \tag{33}$$

Substituting the value of $N(\xi)$ defined by (33) into eqns (19) and (20) we find that

$$I_1(r)+I_2(r)+I_3(r) = 0 \begin{cases} 0<r<a \\ b<r<\infty \end{cases} \tag{34a,b}$$

where

$$I_j(r) = \int \lambda f_j(\lambda) L(r,\lambda)\,\mathrm{d}\lambda\,; \quad (j=1,2,3) \tag{35}$$

$$L(r,\lambda) = \int_0^\infty J_1(\xi r)J_1(\xi\lambda)\,\mathrm{d}\xi \tag{36}$$

and the limits of integration in (35) can occupy the ranges $(0, a)$, (a, b) and (b, ∞) depending upon the value of j.

From the results given by Cooke (1963) we note that

$$L(r,\lambda) = \begin{cases} \dfrac{2}{\pi\lambda r}\displaystyle\int_0^{\min(\lambda,r)} \frac{s^2\,\mathrm{d}s}{[(\lambda^2-s^2)(r^2-s^2)]^{1/2}} \\ \dfrac{2\lambda r}{\pi}\displaystyle\int_{\max(\lambda,r)}^\infty \frac{\mathrm{d}s}{s^2[(s^2-\lambda^2)(s^2-r^2)]^{1/2}} \end{cases} \tag{37}$$

where

$$\int_a^b \mathrm{d}\lambda \int_0^{\min(\lambda,r)} \mathrm{d}s = \int_a^r \mathrm{d}s \int_s^b \mathrm{d}\lambda + \int_0^a \mathrm{d}s \int_a^b \mathrm{d}\lambda \tag{38a}$$

and

$$\int_a^b \mathrm{d}\lambda \int_{\max(\lambda,r)}^\infty \mathrm{d}s = \int_r^b \mathrm{d}s \int_a^s \mathrm{d}\lambda + \int_b^\infty \mathrm{d}s \int_a^b \mathrm{d}\lambda \tag{38b}$$

Using these results the eqn (34a) can be written as

$$\int_0^r \frac{\{F_1(s)+\tilde{F}_2(s)\}\,\mathrm{d}s}{\sqrt{r^2-s^2}} = -r^2\int_b^\infty \frac{F_3(s)\,\mathrm{d}s}{s^2\sqrt{s^2-r^2}};\quad 0<r<a \tag{39}$$

where

$$F_1(s) = s^2\int_s^a \frac{f_1(\lambda)\,\mathrm{d}\lambda}{\sqrt{\lambda^2-s^2}};\quad 0<s<a \tag{40}$$

$$\tilde{F}_2(s) = s^2\int_a^b \frac{f_2(\lambda)\,\mathrm{d}\lambda}{\sqrt{\lambda^2-s^2}};\quad a<s<b \tag{41}$$

$$F_3(s) = \int_b^s \frac{\lambda^2 f_3(\lambda)\,\mathrm{d}\lambda}{\sqrt{s^2-\lambda^2}}\quad b<s<\infty \tag{42}$$

The solution of the Abel integral eqn (39) is given by

$$F_1(s) = -\tilde{F}_2(s)-\frac{2}{\pi}\int_b^\infty \left[-\frac{s^2}{u(s^2-u^2)}+\frac{s}{2u^2}\log_e\left|\frac{s+u}{s-u}\right|\right]F_3(u)\,\mathrm{d}u;\quad 0<s<a \tag{43}$$

Similarly (34b) gives

$$\int_r^\infty \frac{[F_3(s)+F_2^*(s)]}{s^2\sqrt{s^2-r^2}}\mathrm{d}s = -\frac{1}{r^2}\int_0^a \frac{F_1(s)\,\mathrm{d}s}{\sqrt{r^2-s^2}} \tag{44}$$

where

$$F_2^*(s) = \int_a^b \frac{\lambda^2 f_2(\lambda)\,\mathrm{d}\lambda}{\sqrt{s^2-\lambda^2}} \tag{45}$$

Again, the solution of the Abel integral eqn (44) is given by

$$F_3(s) = -F_2^*(s)-\frac{2}{\pi}\int_0^a F_1(u)\left\{\frac{s}{(s^2-u^2)}+\frac{1}{2u}\log_e\left|\frac{s+u}{s-u}\right|\right\}\mathrm{d}u;\quad b<s<\infty \tag{46}$$

Also considering (27), (28), (31) and (32) we can show that

$$\varphi_1(t) = \frac{32G\delta(1-\nu)}{(7-8\nu)\pi}+\frac{2}{\pi(7-8\nu)}\int_0^a \frac{\varphi_2(u)(u^2-2t^2)H(u-t)\,\mathrm{d}t}{u\sqrt{u^2-t^2}}$$
$$+\frac{8(1-2\nu)}{(7-8\nu)\pi^2}\left\{\int_0^a \frac{F_1(s)\,\mathrm{d}s}{(s^2-t^2)}+\frac{\pi}{2}\int_a^b F_2(s)\,\mathrm{d}s+\frac{\pi}{2}\int_b^\infty \frac{F_3(s)}{s^2}\mathrm{d}s\right\};\quad 0<t<a \tag{47}$$

where $H(x)$ is the Heaviside unit function. Substituting the value of $M(\xi)$ from (28) into (18) we obtain

$$\int_0^a t\varphi_2(t)K(r,t)\,\mathrm{d}t = \int_0^\infty \frac{1}{(7-8v)}\{L(\xi)+2(1-2v)N(\xi)\}J_2(\xi r)\,\mathrm{d}\xi\,; \quad 0<r<a \tag{48}$$

where

$$K(r,t) = \frac{2}{\pi(rt)^2}\int_0^{\min(r,t)} \frac{s^4\,\mathrm{d}s}{[(t^2-s^2)(r^2-s^2)\}^{1/2}} \tag{49}$$

Also, introducing the substitution

$$P(s) = \int_s^a \frac{\varphi_2(t)\,\mathrm{d}t}{t(t^2-s^2)^{1/2}}\,; \quad 0<s<a \tag{50}$$

and using the representations for $L(\xi)$ and $N(\xi)$ it can be shown that

$$P(s) = -\frac{\pi}{2s(7-8v)}\left[\frac{\varphi_1(s)}{s}-\frac{1}{s^2}\int_0^s \varphi_1(t)\,\mathrm{d}t\right]+\frac{2(1-2v)}{\pi s^3(7-8v)}\int_0^a \frac{F_1(u)}{u}\log_e\left|\frac{u+s}{u-s}\right|\mathrm{d}u$$
$$-\frac{4(1-2v)}{\pi(7-8v)s^2}\int_0^a \frac{F_1(u)}{(u^2-s^2)}\,\mathrm{d}u\,; \quad 0<s<a \tag{51}$$

Finally, the eqn (47) can be reduced to the form

$$\varphi_1(t) = \frac{32G\delta(1-v)}{(7-8v)\pi^2}+\frac{2}{(7-8v)\pi}\int_0^a sP(s)H(s-t)\,\mathrm{d}s$$
$$-\frac{2t^2P(t)}{(7-8v)\pi}+\frac{8(1-2v)}{(7-8v)\pi^2}\left\{\int_0^a \frac{F_1(s)\,\mathrm{d}s}{(s^2-t^2)}+\frac{\pi}{2}\int_a^b F_2(s)\,\mathrm{d}s+\frac{\pi}{2}\int_b^\infty \frac{F_3(s)\,\mathrm{d}s}{s^2}\right\}; \quad 0<t<a \tag{52}$$

Considering (23) and (32) we have

$$f_2(r) = -\frac{(1-2v)}{2}\int_0^\infty \xi[L(\xi)+M(\xi)]J_1(\xi r)\,\mathrm{d}\xi\,; \quad a<r<b \tag{53}$$

Using the values for $L(\xi)$ and $M(\xi)$, defined by (27) and (28), in (53) we obtain

$$f_2(r) = \frac{(1-2v)}{2}\left[\frac{2}{\pi r}\int_0^a \frac{\varphi_2(t)}{t}\,\mathrm{d}t\int_0^t \frac{s^4\,\mathrm{d}s}{(t^2-s^2)^{1/2}(r^2-s^2)^{3/2}}+r\int_0^a \frac{\varphi_1(t)\,\mathrm{d}t}{(r^2-t^2)^{3/2}}\right]; \quad a<r<b \tag{54}$$

Re-ordering the double integral in (54) and using the result (50) we can write (54) as

$$f_2(r) = \frac{(1-2v)}{\pi r}\int_0^a \frac{s^4P(s)\,\mathrm{d}s}{(r^2-s^2)^{3/2}}-\frac{(1-2v)r}{2}\int_0^a \frac{\varphi_1(t)\,\mathrm{d}t}{(r^2-t^2)^{3/2}}\,; \quad a<r<b \tag{55}$$

The mixed boundary value problem related to the embedded disc inclusion problem defined by eqns (11)–(16) is now reduced to the solution of the coupled integral eqns (43), (46), (51), (52) and (55) for the unknown functions $F_1(s)$, $F_3(s)$, $f_2(r)$, $P(s)$ and $\varphi_1(t)$. The structure of these coupled integral equations is such that results of practical interest can be obtained only upon numerical solution of these equations.

4. Load–displacement behaviour of the disc inclusion

The shear stress distribution at the disc inclusion–elastic medium interfaces can be used to evaluate the in-plane load–displacement relationship for the rigid disc inclusion. The shear traction on the plane $z = 0$ in the x-direction is given by

$$T_x = (\sigma_{rz}\cos\theta - \sigma_{\theta z}\sin\theta) = -\frac{1}{2}\int_0^\infty \xi L(\xi) J_0(\xi r)\,\mathrm{d}\xi\,; \quad 0 < r < a \tag{56}$$

The resultant force T required to induce the in-plane displacement δ is given by

$$T = -2\pi \int_0^a r\,\mathrm{d}r \int_0^\infty \xi L(\xi) J_0(\xi r)\,\mathrm{d}\xi \tag{57}$$

Since

$$\int_0^\infty \xi(L)(\xi) J_0(\xi r)\,\mathrm{d}\xi = \frac{\varphi_1(a)}{\sqrt{a^2-r^2}} - \int_r^a \frac{\varphi_1'(t)\,\mathrm{d}t}{\sqrt{t^2-r^2}} \tag{58}$$

where the prime indicates the derivative with respect to t, (57) can be reduced to the result

$$T = -2\pi \int_0^a \varphi_1(t)\,\mathrm{d}t \tag{59}$$

5. Stress intensity factor at the crack tip

Since the state of deformation induced in the elastic medium as a result of the displacement of the inclusion is symmetric about the plane $z = 0$, the mode II and mode III stress intensity factors at the boundary of the crack are identically zero. The non-zero mode I stress intensity factor at the boundary of the crack can be obtained by considering the axial stress $\sigma_{zz}(r, 0)$ in the region $r > b$. Using the result (8), the substitutions (24), (25), (28) and the expressions (27), (33) and (37) we obtain

$$\begin{aligned}\frac{4(1-\nu)}{(1-2\nu)}\sigma_{zz}(r,0,0) &= \frac{a\varphi_1(a)}{r\sqrt{r^2-a^2}} - \frac{1}{r}\int_0^a \frac{\varphi_1'(t)\,\mathrm{d}t}{(r^2-t^2)^{1/2}} \\ &+ \frac{4}{\pi r(1-2\nu)}\int_b^r \frac{F_3(s)\,\mathrm{d}s}{s(r^2-s^2)^{1/2}} + \frac{2}{(1-2\nu)}\left[\frac{2rF_3(b)}{\pi b^2\sqrt{r^2-b^2}} + \frac{2r}{\pi}\int_b^r \left(\frac{F_3(s)}{s^2}\right)' \frac{\mathrm{d}s}{(r^2-s^2)}\right] \\ &- \frac{2}{\pi r}\int_0^a \frac{\varphi_2(t)\,\mathrm{d}t}{t}\int_0^t \frac{s^4\,\mathrm{d}s}{[(t^2-s^2)^{1/2}(r^2-s^2)^{3/2}]}; \quad r > b\end{aligned} \tag{60}$$

where the prime denotes the derivative with respect to the appropriate argument. The stress intensity factor at $r = b$ is defined by

$$K_{\mathrm{I}}^{b} = \lim_{r \to b^{+}} [2(r-b)]^{1/2} \sigma_{zz}(r, 0, 0) \tag{61}$$

Using the result (60) in (61) we have

$$K_{\mathrm{I}}^{b} = \frac{1}{\pi(1-\nu)} \frac{F_3(b)}{b^{3/2}} \tag{62}$$

It is noted that the mode I stress intensity factor given by (62) is evaluated only at the location $\theta = 0$. From (8) it is evident that σ_{zz} has a variation in θ which is proportional to $\cos\theta$ and we further assume that the definition of the stress intensity factor is valid for $\theta \varepsilon (\pi/2, 3\pi/2)$.

6. Numerical results

We adopt a numerical technique for the solution of the coupled system of integral eqns (43), (46), (51), (52) and (55) for the unknown functions $F_1(s)$, $F_3(s)$, $f_2(r)$, $P(s)$ and $\varphi_1(t)$. The general procedures for the solution of this class of integral equations are given by Baker (1978) and further applications are also given by Selvadurai (1993, 1994a, b) and Selvadurai et al. (1990, 1991). The intervals involved are $(0, a]$, $[a, b]$ and $(b, \infty]$. If N_1, N_2 and N_3 segments are considered, then we can define the locations, given by,

$$x_i = (i-1)h_1 \quad \text{with } i = 1, 2, \ldots, N_1 + 1 \tag{63}$$

$$y_i = a + (i-1)h_2 \quad \text{with } i = 1, 2, \ldots, N_2 + 1 \tag{64}$$

and

$$z_i = z_{i-1} + \alpha(z_{i-1} - z_{i-2}) \quad \text{with } i = 3, 4, \ldots, N_3 + 1 \tag{65}$$

where $h_1 = a/N_1$, $h_2 = (b-a)/N_2$; $z_1 = b$; $z_2 = b + h_2$ and α is a constant of proportionality such that the interval $(b, \infty]$ is approximated in the numerical scheme. Using the above discretization, the governing integral equations can be written in the form of a matrix equation

$$[A_{ij}]\{X_j\} = \{F_i\} \tag{66}$$

where $i, j = 1, 2, \ldots, N$ and $N = 3N_1 + N_2 + N_3$. The matrix $[A_{ij}]$ in (66) are the kernel coefficients in the five integral equations and $\{X_j\}$ are the values of the unknown functions at the collocation points. The right-hand side of (66) is given as

$$\{F_i\} = \begin{cases} 1 & \text{if } i = N_1 + 1, \ldots, 2N_1 \\ 0 & \text{for all other } i \end{cases} \tag{67}$$

The resultant force on the inclusion can be determined from the function $\varphi_1(t)$ in (52) and the result (59). We have

$$\frac{T}{64(1-\nu)G\Delta a/(7-8\nu)} = -\frac{1}{N_1}\sum_{j=N_1+1}^{2N_1} X_j \tag{68}$$

The stress intensity factor defined by (62) and applicable to $0 < \theta < 2\pi$, can be expressed in the form

$$K_{\mathrm{I}}^{b} = \frac{32G\Delta\cos\theta}{(7-8\nu)\pi^2 b^{3/2}} X_{N-N_3+1} \tag{69}$$

This result can be normalized with respect to either the stress intensity factor at the boundary of a penny-shaped crack subjected to in-plane point loads of equal magnitude $T/2$ acting in the x-direction, i.e.

$$[K_{\mathrm{I}}^{b}]_{\text{point load}} = \frac{T(1-2\nu)\cos\theta}{8\pi(1-\nu)b^{3/2}} \tag{70}$$

or with respect to the case when $a \to b$; i.e.

$$[K_{\mathrm{I}}^{b}]_{a\to b} = \frac{16G\Delta a(1-2\nu)\cos\theta}{(7-8\nu)\pi^2 b^{3/2}} \tag{71}$$

Figure 2 illustrates the variation in the in-plane stiffness of the disc inclusion as determined from the numerical procedure described previously.

In the limit as $(a/b) \to 0$ (with $a \neq 0$), the problem corresponds to the in-plane loading of a disc inclusion which is embedded between two-halfspace regions and subjected to an in-plane force T. The analytical solution to this problem can be obtained from the results developed for the in-plane translation of a rigid punch bonded to an isotropic elastic halfspace (see e.g. Gladwell, 1980); i.e.

$$T = \frac{16G\Delta a}{\left\{1 + \dfrac{(1-2\nu)}{\ln(3-4\nu)}\right\}} \tag{72}$$

The analytical result for the in-plane stiffness given by (72) exactly matches the numerical result when $\nu = 1/2$ and when $\nu = 0$, the discrepancy between the analytical and numerical solutions is approximately 0.4%.

Figure 3 illustrates the variation in the crack opening mode stress intensity factor [normalized with respect to the limiting value defined by (71)] as a function of the inclusion-crack aspect ratio a/b and Poisson's ratio. As the diameter of the inclusion reduces to zero (with T being finite), the result reduces to the case where the crack is subjected to symmetrically directed forces of equal magnitude $T/2$ which act along the x-direction.

7. Conclusions

The problem related to the in-plane translation of a penny-shaped rigid disc which is embedded in bonded contact within a penny-shaped crack can be examined by formulating the problem as a

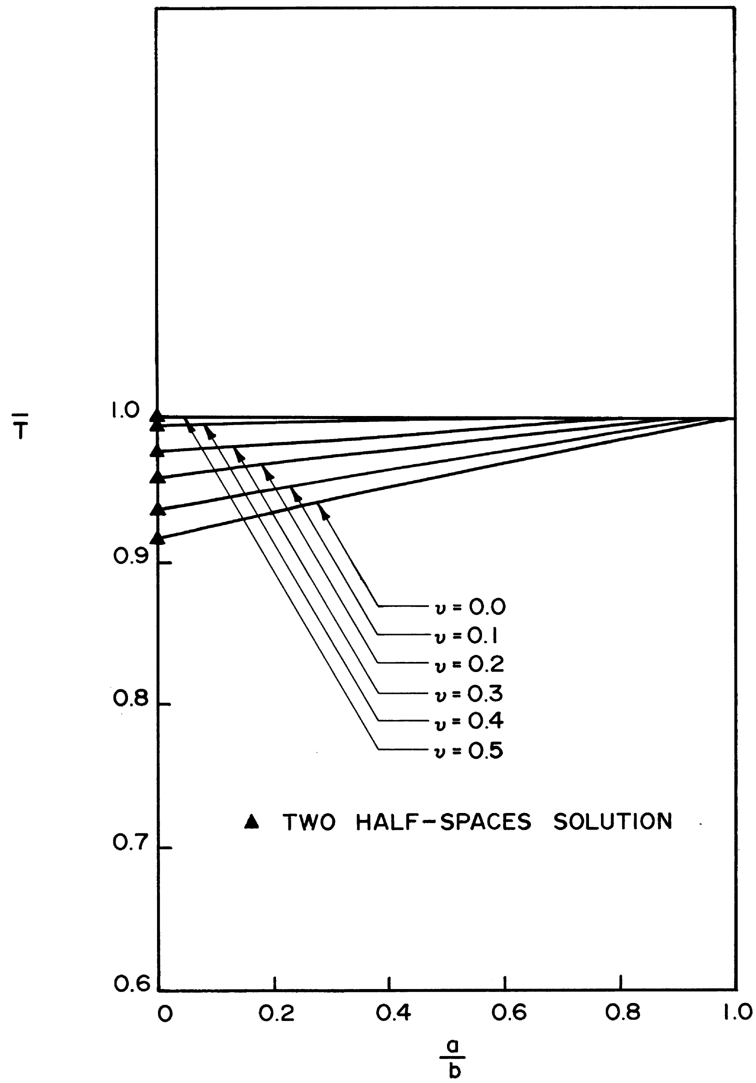

Fig. 2. The influence of the inclusion-crack aspect ration (a/b) on the in-plane stiffness of the disc inclusion
$$\left[\bar{T} = \frac{T(7-8\nu)}{64G\Delta a(1-\nu)}\right].$$

mixed boundary value problem referred to a halfspace region. It is shown that the mixed boundary value problem can be reduced to a system of coupled integral equations which can be solved by using a quadrature scheme, to develop results of engineering interest. In the case when the inclusion is bonded to the surfaces of the crack, the stress singularity at the boundary of the inclusion will exhibit an oscillatory form of a stress singularity. Studies conducted previously in connection with

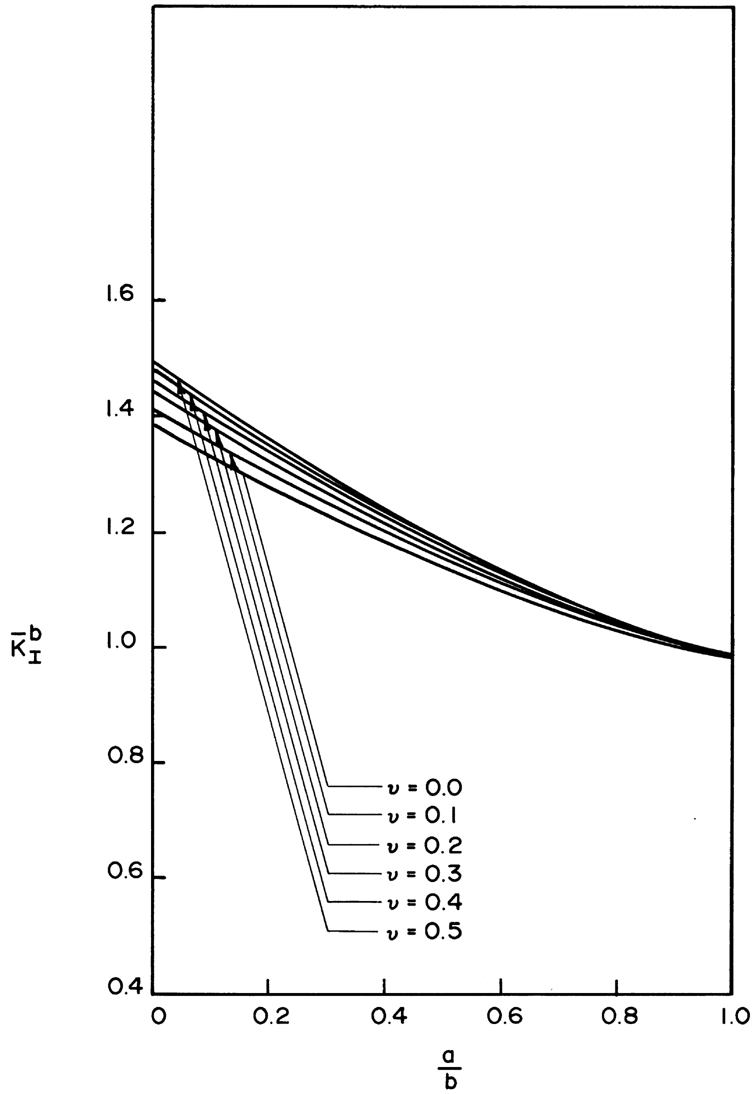

Fig. 3. The influence of the inclusion-crack aspect ration (a/b) on the mode I stress intensity factor at the crack tip $r = b$

$$\left[\bar{K}_{\mathrm{I}}^{b} = \frac{K_{\mathrm{I}}^{b}(7-8\nu)\pi^{2}b^{3/2}}{16G\Delta a(1-2\nu)\cos\theta}\right].$$

the axial loading of an inclusion embedded in a crack have shown that such local effects have very little influence on the overall responses such as the load–displacement behaviour of the inclusion. The stress singularity at the crack tip is regular and the nonzero axial stress can be used to compute the mode I stress intensity factor. Furthermore, the numerical results indicate that the in-plane stiffness of the inclusion is not significantly influenced by the extent of cracking in the plane of the inclusion. For all practical purposes, the elastic solution can be conveniently computed by making use of the exact analytical result for the in-plane translation of a rigid punch which is embedded in bonded contact between two halfspace regions.

References

Baker, C.T.H., 1978. The Numerical Treatment of Integral Equations. Oxford University Press, Oxford, U.K.

Collins, W.D., 1962. Some axially symmetric stress distributions in elastic solids containing penny-shaped cracks. I. Cracks in an infinite solid and a thick plate. Proc. Roy. Soc. A203, 359–386.

Cooke, J.C., 1963. Triple integral equations. Q. J. Mech. Appl. Math. 16, 193–203.

Gladwell, G.M.L., 1980. Contact Problems in the Classical Theory of Elasticity. Sijthoff and Noordhoff, The Netherlands.

Kassir, M.K., Sih, G.C., 1968. Some three-dimensional inclusion problems in elasticity theory. Int. J. Solids Struct. 4, 225–241.

Keer, L.M., 1965. A note on the solution of two asymmetric boundary value problems. Int. J. Solids Struct. 1, 257–264.

Muki, R., 1960. Asymmetric problems of the theory of elasticity for a semi-infinite solid and a thick plate. In: Sneddon, I.N., Hill, R. (Eds.), Progress in Solid Mechanics. North-Holland, Amsterdam, 1, 339–349.

Mura, T., 1981. Micromechanics of Defects in Solids. Sijthoff and Noordhoff, The Netherlands.

Mura, T., 1988. Inclusion problems. Applied Mechanics Reviews 41, 15–20.

Selvadurai, A.P.S., 1989. The influence of boundary fracture of the elastic stiffness of a deeply embedded anchor plate. Int. J. Num. Analy. Meth. Geomech. 13, 159–170.

Selvadurai, A.P.S., 1993. The axial loading of a rigid circular anchor plate embedded in an elastic halfspace. Int. J. Num. Analyt. Meth. Geomech. 17, 343–353.

Selvadurai, A.P.S., 1994a. Analytical methods for embedded flat anchor problems in geomechanics. In: Siriwardane, H.J., Zaman, M.M. (Eds.), Computer Methods and Advances in Geomechanics. Proc. 8th Int. Conf. on Computer Meth. Adv. Geomech., Morgantown, W. VA., 1, 305–321.

Selvadurai, A.P.S., 1994b. On the problem of a detached anchor plate embedded in a crack. Int. J. Solids Struct. 31, 1279–1290.

Selvadurai, A.P.S., Au, M.C., Singh, B.M., 1990. Asymmetric loading of an externally cracked elastic solid by an in-plane penny-shaped inclusion. Theor. Applied Fracture Mech. 14, 253–266.

Selvadurai, A.P.S., Singh, B.M., Au, M.C., 1991. The in-plane loading of a rigid disc inclusion embedded in an elastic halfspace. J. Appl. Mech. 58, 1–8.